

Probing the light induced dipole-dipole interaction in momentum space

R. LÖW¹, R. GATI², J. STUHLER¹ and T. PFAU¹

¹ *5. Physikalisches Institut, Universität Stuttgart, 70550 Stuttgart*

² *Kirchhoff Institut, Universität Heidelberg, 69120 Heidelberg*

PACS. 42.50.Ct – Quantum description of interaction of light and matter.

PACS. 34.20.Cf – Interatomic potentials and forces.

PACS. 03.75.-b – Matter waves.

Abstract. –

We theoretically investigate the mechanical effect of the light-induced dipole-dipole interaction potential on the atoms in a Bose-Einstein condensate. We present numerical calculations on the magnitude and shape of the induced potentials for different experimentally accessible geometries. It is shown that the mechanical effect can be distinguished from the effect of incoherent scattering for an experimentally feasible setting.

Introduction. – The interaction of a radiation field with an ensemble of atoms has been investigated in many distinct contexts since the early works of Lorentz and Lorenz [1] of light in dense media. Within one century, researchers came up with an innumerable variety of light-matter interaction types [2] and reached a recent summit with the development of laser cooling [3]. The dipole character of an atom, driven by an electromagnetic wave, can be used to apply forces on atoms by intensity gradients of light fields [4] but it can also produce forces between atoms [5]. The implication of interacting atoms on the refractive index was treated theoretically for dilute Bose gases [6] with an extended Lotentz-Lorenz model. The effect of light-induced or excited state collisions shows up in laser cooling by losses in magneto-optical traps [7]. The coherent part of this interaction is recently discussed in basically two directions. The one focuses on the properties of the light absorbed and emitted in dense media, namely radiation trapping [8], level shifts [9], dipole blockade effects as a tool for quantum information processing [10] and collective effects such as superradiance [11]. The other main focus tends towards new forms of interaction in Bose-Einstein condensates as effective $1/r$ potentials [12] or as a generator for rotons [13]. Recently, the effect of the resonant dipole-dipole interaction in a cold cloud of highly excited Rydberg states was observed by broadening of spectroscopic lines [14] and by resonant energy transfer between different Rydberg states [15].

In this letter, we investigate new physical aspects that arise in dense cold atomic samples irradiated by a near resonant laser beam. Atoms exposed to an electromagnetic wave responds as damped harmonic oscillators and exhibit an alternating electric dipole moment. The interaction energy of such dipoles can exceed the one of magnetic dipoles in atomic ground states

by several orders of magnitude. We propose and theoretically investigate an experiment which allows to study the coherent interaction of laser induced electric dipoles by transferring the interaction energy among the dipoles into kinetic energy, which can be probed with standard time of flight techniques. Initially, the dipoles are generated for a certain flash time by a laser beam with linear polarization in a spin polarized sample of cold atoms. During the flash time, the dipole moments reach a steady state and the light-induced dipole-dipole interaction potential is build up. As a first step, we calculate this potentials for a certain density distribution including the retardation effects of the dipolar fields and the driving electromagnetic wave. The flash time is chosen long enough that the atoms can evolve in the induced potential, namely to gain momentum, but short enough not to change the initial density distribution. As a next step we discuss the increase of the initial momentum distribution for different geometries of the atomic cloud and as a function of the angle of the linear polarization of the laser light. Finally, the results are compared with parasite effects like spontaneous scattering.

Outline of the calculation. – In the following, we are dealing with oscillating dipoles driven by an electromagnetic wave with linear polarization and wave vector k . We assume that all dipole moments are of equal strength, oriented parallel and oscillate with the same frequency. The phase between two dipoles depends on the position of the atoms with respect to the electromagnetic wave phase fronts and the interatomic distance. The retarded interaction potential for two interacting dipoles with one dipole located at the origin and the other at \vec{r}_0 reads [16]

$$\tilde{V}_{\text{dd}}(\vec{r}_0, 0) = \frac{d^2 \cos(\vec{k} \cdot \vec{r}_0)}{4\pi\epsilon_0 r_0^3} \cdot \sum_{i,j} [(\delta_{ij} - 3\frac{r_{0,i}r_{0,j}}{r_0^2})(\cos(kr_0) + kr_0 \sin(kr_0)) - (\delta_{ij} - \frac{r_{0,i}r_{0,j}}{r_0^2})(k^2 r_0^2 \cos(kr_0))] \quad i, j = x, y, z \quad (1)$$

where d is the absolute value of the dipole moment and \vec{k} the wave vector of the driving field. Finally, we want to look at a system of N pairwise interacting dipoles with a density distribution $n(\vec{r})$. The superposed potential for a dipole at position \vec{r}_0 is given by

$$V_{\text{dd}}(\vec{r}_0) = \int \tilde{V}_{\text{dd}}(\vec{r}_0, \vec{r}) n(\vec{r}) d^3r. \quad (2)$$

Replacing $\tilde{V}_{\text{dd}}(\vec{r}_0, \vec{r})$ by $d^2 \cos(\vec{k} \cdot (\vec{r}_0 - \vec{r})) V'_{\text{dd}}(\vec{r}_0 - \vec{r})$, it is possible to rewrite the integral as a convolution

$$V_{\text{dd}}(\vec{r}_0) = \int d^2 \cos(\vec{k} \cdot (\vec{r}_0 - \vec{r})) V'_{\text{dd}}(\vec{r}_0 - \vec{r}) n(\vec{r}) d^3r \quad (3)$$

to which the convolution theorem can be applied. Since there exists no analytical solution, we discretize the integral (3) on a simple cubic lattice and use FFT algorithms for evaluation.

The induced dipole potential V_{dd} changes the momentum distribution of the atomic cloud. In the following, we assume a density distribution of a Bose-Einstein condensate with all atoms having the same phase. The undisturbed wave function can be written as $\psi_0(\vec{r}) = e^{i\varphi(t)} \sqrt{n_0(\vec{r})}$. The wave function is an eigen-state of the unperturbed situation and therefore the time evolution operator of the system, after the interaction is switched on, writes $\hat{U}(\vec{r}, t) = \exp(-iV_{\text{dd}}(\vec{r})t/\hbar)$ and with this $\psi(\vec{r}, t) = \hat{U}(\vec{r}, t)\psi_0(\vec{r})$. Here we demand that the density distribution does not change during the interaction time, which is legitimate in the so called Raman Nath regime. The Raman-Nath approximation is valid as long the gained kinetic

energy is much smaller than the interaction potential. The momentum distribution after the interaction time t is given by

$$\tilde{n}(\vec{k}, t) = \left| \int e^{i\vec{k}\vec{r}} \hat{U}(\vec{r}, t) \psi_0(\vec{r}, 0) d^3r \right|^2 / 8\pi^3. \quad (4)$$

To evaluate the magnitude of the dipole moment, we consider the atoms as two level systems driven by a coherent light field. This system has a steady state dipole moment, which arises from a superposition of the atomic ground and excited state. The amplitude of this oscillating dipole can be derived using optical Bloch equations [17]. The steady state dipole moment reads

$$d = 2 \frac{d_{ge}}{\Omega} \frac{s}{s+1} \sqrt{\delta^2 + \Gamma^2/4} \quad (5)$$

where d_{ge} is the dipole matrix element, $\Omega = \Gamma \sqrt{I_0/2I_{\text{sat}}}$ the Rabi frequency, Γ the natural linewidth, δ the laser detuning from resonance and the saturation parameter

$$s = \frac{I_0}{I_{\text{sat}}} \frac{1}{1 + 4(\delta/\Gamma)^2}. \quad (6)$$

I_0 is the intensity of the flashing laser and $I_{\text{sat}} = \pi \hbar c \Gamma / 3 \lambda^3$ the saturation intensity. A maximum dipole moment only depends on atomic parameters

$$d_{\text{max}} = \sqrt{\frac{3 \Gamma \epsilon_0 \hbar c^3}{4 \omega_0^3}} \quad (7)$$

and is reached for any detuning if the intensity is set to $I_0 = I_{\text{sat}} (1 + 4\delta^2/\Gamma^2)$ with ω_0 being the transition frequency. The maximum dipole moment coincides with a saturation parameter of one and therefore the spontaneous scattering rate is fixed to $\Gamma/4$.

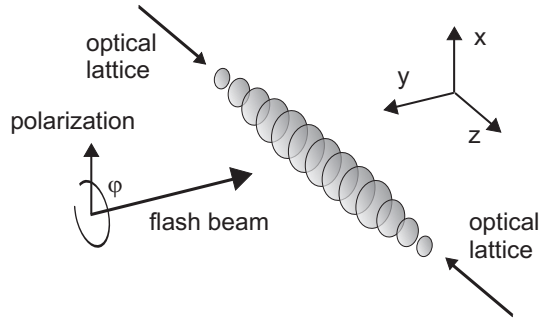


Fig. 1 – A Bose-Einstein condensate within an one-dimensional optical lattice. The resulting density distribution is a stack of pancake-shaped condensates. A laser along the y -direction induces the dipole-dipole interaction. The linear polarization of the flash beam can be altered from x -polarization ($\varphi=0^\circ$) to z -polarization ($\varphi=90^\circ$). The altered momentum distribution is either projected onto the x - z plane or the y - z plane.

Numerical calculations-realistic experimental setups. – To illustrate the mechanical effect of the dipole-dipole interaction, we choose a specific example which corresponds to parameters that are realistic in a typical Bose-Einstein condensate experiment with Rb^{87} atoms

in the $F=2$, $m_F=2$ ground state. The atomic cloud is confined in a cigar-shaped magnetic trap with the long axes along z as depicted in fig. 1. In addition, we adiabatically switch on a retroreflected laser beam at 785nm to create an optical lattice along the z -axis to increase the density. The depth of the lattice is set to 100 recoil energies, which results in an axial trapping frequency of 105 kHz. The additional axial confinement due to the magnetic trap is neglected. Radially, the trapping frequency is set to 1 kHz. Due to the strong axial confinement, the density distribution of the ground state can not be calculated in the Thomas-Fermi approximation. We solved the full Gross-Pitaevskii equation [18] numerically with an imaginary time Schrödinger equation for 250 atoms in a single lattice site for the given trapping frequencies. The resulting pancake-shaped density distribution can be approximated in radial direction by a parabola with a Thomas-Fermi radius of $1.15 \mu\text{m}$ and axially by an Gaussian distribution with a $1/e^2$ radius of 34.2 nm. The resulting peak density is $9.7 \times 10^{20} \text{ m}^{-3}$ and the chemical potential is 5.8 kHz. In the following, we assume an infinite stack of equal pancakes separated by $\lambda/2=785/2$ nm. The calculation is carried out initially on a single pancake and is finally superposed according to the infinite stack. The grid for the numerical calculation is chosen to be $64 \times 64 \times 128 = 65.536$ lattice points and the grid lattice spacing is $\lambda_{ol}/32 = 24.5$ nm where λ_l is the wavelength of the laser generating the optical lattice. The direction of the detuning of the laser affects only slightly the lattice constant and with this the superposition of the constituent potentials of each pancake.

The intensity of the flash beam is set to $1120 I_{\text{sat}}$ and its frequency is detuned 100 MHz from the $F=2$ to $F=3$ transition (D2 multiplet of Rubidium) at 780.249 nm, which corresponds to a detuning of 16.7Γ . Using such a large detuning, one can neglect an inhomogeneous illumination of the atomic cloud since only a small fraction of the light is absorbed. The induced dipole potentials alters the effective detuning to the flash beam which results in an altering phase and magnitude of the oscillating dipoles within the cloud. This effect can also be neglected, since the detuning of the flash beam is much larger than the induced dipole potential. Also nonlinear effects as lensing by the inhomogeneous density distribution and radiation trapping are strongly suppressed. The flash beam propagates along the y -direction and its polarization angle φ can be altered from 0° (polarization along the x -axis) to 90° (polarization along the z -axis). The steady state dipole moment with this parameters is 5.26 Debye. The flash time was set to 300 ns, long compared to $1/\Gamma$, so that all dipoles are in a steady state, but short enough for being in Raman Nath regime. This means also that superradiant effects can be neglected [19]. The atoms are initially prepared in the $F=2, m_F=2$ state in respect to the z -axis.

To account for additional broadening effects of the momentum distribution by spontaneous scattering events, the time evolution of the full atomic density matrix was carried out. This includes the different polarizations of the driving field, the pumping of the atoms into other m_F states and the angular distribution of the acquired recoil. For given parameters, about three photons are scattered per atom. The amount of scattered photons can be experimentally checked for consistency purposes by the shift of the center of mass position after some time of flight of the atom cloud.

The final momentum distribution is given by the convolution of the momentum gain due to the induced dipole potential, the mean field of the Bose-Einstein condensate and the spontaneously scattered photons. To extract a mean momentum broadening, the convoluted distribution was fitted with very good agreement by Gaussian distribution.

Results. – In fig. 2 the distribution of the light-induced dipole-dipole interaction potential through the center of a pancake along the y -axis is shown. The contribution of the neighbouring pancakes is included by periodic boundary conditions. The different curves rep-

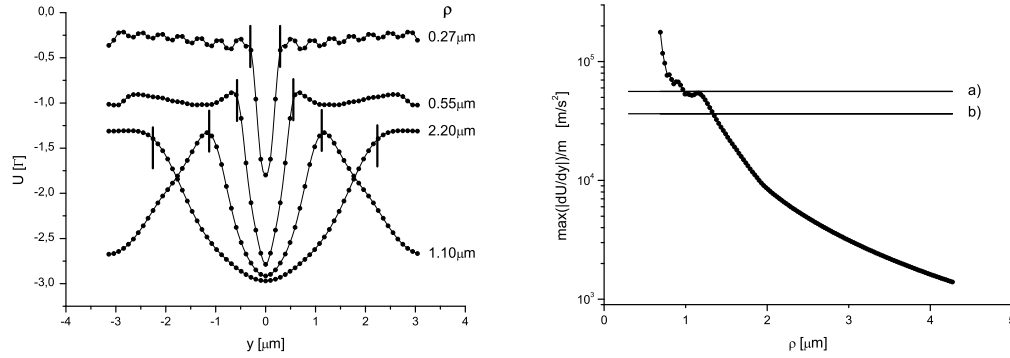


Fig. 2 – The left figure shows the induced potentials along the y -axes at $x=z=0$ for different radial widths ρ of the atomic clouds. The numbers and the vertical bars at each plot indicate the radial Thomas-Fermi radius. The peak atomic density was kept constant at $9.7 \times 10^{20} \text{m}^{-3}$ for all widths. The polarization of the flash beam points always along the x -axis. On the right side, the maximum acceleration as dependence of the radial Thomas-Fermi radius ρ is depicted. The data shows the maximum gradient of the potentials divided by the mass of a Rubidium atom ($m=1.44 \times 10^{-25} \text{kg}$). The horizontal line a) gives an upper limit for the unidirectional acceleration ($\frac{d\langle p \rangle}{dt}/m = \hbar k \Gamma / 4m$) due to radiation pressure. The horizontal line b) marks the maximum acceleration due to momentum diffusion caused by spontaneous emission processes ($\frac{d\sqrt{\langle p^2 \rangle}}{dt}/m$). The flashing laser has a detuning of 100 MHz and an intensity of $1120 I_{\text{sat}}$.

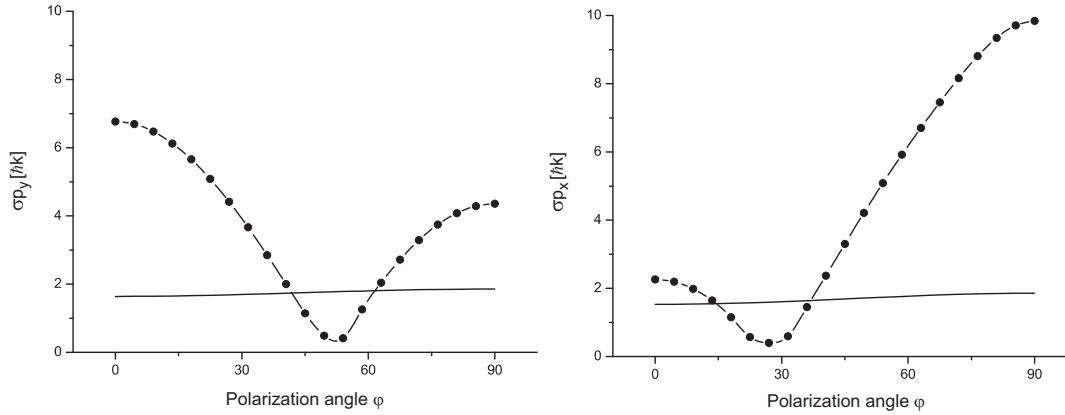


Fig. 3 – The two graphs depict the width of the momentum distribution of the atomic cloud after the light-induced dipole-dipole potential was applied for 300ns. The Thomas Fermi radius was set to $1.15 \mu\text{m}$. The graph on the left shows the broadening in momentum space projected onto the y -axes as a function of the polarization angle and the right the projection onto the x -axes. The slash-dotted line includes the effect of the light-induced potentials and the chemical potential. The solid line is the incoherent background of the spontaneously scattered photons as a function of the polarization angle ϕ . To receive the full width in momentum space one has to add the two curves in quadrature.

resent pancakes with different radial sizes but at fixed axial size and constant density and show the dependence of the induced potentials on the geometry of the atomic cloud. In the limit of an infinite cloud with a constant density distribution, the potential would be just a constant and its mechanical effect on the atoms vanishes. The increase of the induced potentials in the center of the cloud with larger radii arises from the greater atom number within the cloud, since the density is kept constant. The interaction potential is on the order of several MHz, which is large compared to all other energy scales in the system like the trapping frequencies and the chemical potential due to the interaction via s-wave scattering.

The right hand side of fig. 2 shows the maximum acceleration extracted from the potentials. For sufficiently small radial sizes of the atomic cloud, the maximum acceleration prevails the unidirectional acceleration $\frac{\hbar k \Gamma}{4}$ due to the spontaneous light force. This allows to clearly distinguish the effects emerging from the dipole-dipole interaction from spontaneous scattering events.

Finally the slash-dotted curves in fig. 3 show the calculated widths of the momentum distribution for the previous parameters along the x and y direction as a function of the polarization angle. Not included in the slash-dotted curves is the contribution of the spontaneous scattering events represented by the solid lines. The broadening in momentum space can be up to 10 recoils, which is fairly larger than the contribution of the chemical potential. Noticable is the existence of a strong dependence of the broadening on the polarization angle φ . In both directions exists an angle at which the effect of the dipole-dipole interaction nearly vanishes and the momentum distribution is dominated by the released chemical potential. The plot on the left side shows a minimum close to the so-called magic angle at 54.74° where the interaction of two dipoles vanishes. Such a minimum broadening is a clear signature of the dipolar character of the potentials since it can not be explained by other light-atom interaction mechanisms.

Conclusion. – We have identified a new regime of coherent light-atom interaction, where novel coherent mechanical effects due to dipole-dipole interactions are predicted. The calculations show that this mechanical effect of the light-induced potentials can be detected experimentally for realistic experimental parameters. The distinct angular dependence of the polarization of the light field is a clear indication for a dipole-dipole interaction. The numerical treatment of the incoherent background of spontaneously scattered photons show that the signal of the desired mechanical effect is about ten times larger and exhibits not such a characteristic angular dependence. By carrying out the proposed experiment, one gains insight in the physics of coherent dipole-dipole interaction and the feasibility for its usage for quantum information processing [10].

We thank M. Lewenstein and L. Santos for helpful discussions and the DFG for the financial support within the priority program SPP1116.

REFERENCES

- [1] LORENTZ H. A., *Wiedem. Ann.*, **9** (1880) 641, LORENZ L., *ibid.*, **11** (1881) 70.
- [2] BORN M. and WOLF E., *Principles of Optics*, 6. ed. (Cambridge University Press, Cambridge) 1999.
- [3] CHU S., *Rev. Mod. Phys.*, **70** (1998) 685, COHEN-TANNOUDJI C. N., *ibid.*, **70** (1998) 707, PHILLIPS W. D., *ibid.*, **70** (1998) 721.
- [4] ASHKIN A., *Phys. Rev. Lett.*, **24** (1970) 156.
- [5] BURNS M. M. and FOURNIER J. M. and GOLOVCHENKO J. A., *Phys. Rev. Lett.*, **63** (1989) 1233.

- [6] MORICE O. and CASTIN Y. and DALIBARD J., *Phys. Rev. A*, **51** (1995) 3896.
- [7] WALLACE C. D. and DINNEEN T. P. and TAN K. N. and GROVE T. T. and GOULD P. L. , *Phys. Rev. Lett.*, **69** (1992) 897.
- [8] MOLISCH A. F. and OEHR Y. B. P., *Radiation Trapping in Atomic Vapors* (Clarendon Press, Oxford) 1998.
- [9] MAKI J. J. and MALCUIT M. S. and SIPE J. E. and BOYD R. W., *Phys. Rev. Lett.*, **67** (1991) 972.
- [10] LUKIN M. D. and FLEISCHHAUER M. and COTE R. and DUAN L. M. and JAKSCH D. and CIRAC J. I. and ZOLLER P., *Phys. Rev. Lett.*, **87** (2001) 037901.
- [11] DICKE R. H., *Phys. Rev.*, **93** (1954) 99.
- [12] O'DELL D. and GIOVANAZZI S. and KURIZKI G. and AKULIN V. M., *Phys. Rev. Lett.*, **84** (2000) 5687.
- [13] O'DELL D. and GIOVANAZZI S. and KURIZKI G., *Phys. Rev. Lett.*, **90** (2003) 110402.
- [14] AFROUSHEH K. and BOHLOULI-ZANJANI P. and VAGALE D. and MUGFORD A. and FEDOROV M. and MARTIN J.D.D. , *Phys. Rev. Lett.*, **93** (2004) 233001.
- [15] CARROLL T. J. and CLARINGBOULD K. and GOODSSELL A. and LIM M. J. and NOEL M. W. , *Phys. Rev. Lett.*, **93** (2004) 153001.
- [16] CRAIG D. P. and THIRUNAMACHANDRAN T., *Molecular Quantum Electrodynamics* (Dover Publications, Inc.) 1998.
- [17] ALLEN L. and EBERLY J. H., *Optical Resonance and Two-Level Atoms* (Dover Publications, Inc.) 1975.
- [18] DALFOVO F. and GIORGINI S. and PIAEVSKII L. P. and STRINGARI S., *Rev. Mod. Phys.*, **71** (1999) 463.
- [19] SCHNEBLE D. and TORII Y. and BOYD M. and STREED E. W. and PRITCHARD D. E. AND KETTERLE W., *Science*, **300** (2003) 475.